Material selection considerations for coaxial, ferrimagnetic-based nonlinear transmission lines

Article *in* Journal of Applied Physics · February 2013

DOI: 10.1063/1.4792214

CITATIONS
23

READS
415

3 authors, including:

James C Dickens
Texas Tech University
443 PUBLICATIONS **2,655** CITATIONS
SEE PROFILE

Andreas A Neuber
Texas Tech University
444 PUBLICATIONS **2,786** CITATIONS
SEE PROFILE

JOURNAL OF APPLIED PHYSICS **113**, 064904 (2013)

Material selection considerations for coaxial, ferrimagnetic-based nonlinear transmission lines

J.-W. B. Bragg, J. C. Dickens, and A. A. Neuber
Center for Pulsed Power and Power Electronics, Department of Electrical & Computer Engineering, Texas Tech University, Lubbock, Texas 79409, USA

(Received 20 December 2012; accepted 30 January 2013; published online 12 February 2013)

The growing need for solid-state high power microwave sources has renewed interest in nonlinear transmission lines (NLTLs). This article focuses specifically on ferrimagnetic-based NLTLs in a coaxial geometry. Achieved peak powers exceed 30 MW at 30 kV incident voltage with rf power reaching 4.8 MW peak and pulse lengths ranging from 1–5 ns. The presented NLTL operates in S-band with the capability to tune the center frequency of oscillation over the entire 2–4 GHz band and bandwidths of approximately 30%, placing the NLTL into the ultra-wideband–mesoband category of microwave sources. Several nonlinear materials were tested and the relationship between NLTL performance and material parameters is discussed. In particular, the importance of the material's ferromagnetic resonance linewidth and its relationship to microwave generation is highlighted. For a specific nonlinear material, it is shown that an optimum relation between incident pulse magnitude and static bias magnitude exists. By varying the nonlinear material's bias magnetic field, active delay control was demonstrated. © *2013 American Institute of Physics*. [http://dx.doi.org/10.1063/1.4792214]

I. INTRODUCTION

The idea of nonlinear transmission lines is not new and traditionally NLTLs, especially coaxial, ferrimagnetic-based, aided slower switches with the ability to provide sub-nanosecond risetime outputs with several nanosecond rise-time inputs.[1,2] Recently, NLTLs have gained more attention as possible solutions to fill the need for high power, compact, and solid-state microwave sources. The NLTL is not limited to coaxial, ferrite-based systems, but encompasses several geometries and modes of operation. A NLTL can be realized in stripline, parallel-plate, microstrip, and lumped element geometries in addition to a coaxial geometry.[3–6] All geometries rely on semiconductors, nonlinear dielectrics, and/or ferrimagnetics, but produce microwaves through different means, i.e., damped gyromagnetic precession, soliton formation, and synchronous wave operation. Frequencies scale from hundreds of MHz up to hundreds of GHz, but come with an inverse relation between rf power (single cycle peak power) and frequency.[7] The coaxial, ferrimagnetic NLTL (from here forth, simply called NLTL) operates through the production of a shockwave followed by damped gyromagnetic precession. Two of the main determining factors of successful microwave generation are the magnetic loss tangent and internal magnetic field of the sample; therefore, this article details the principles of operation and effects of material properties and magnetic fields (both incident pulse and static bias) on the overall microwave performance of NLTLs.

II. BACKGROUND

Several mechanisms contribute to pulse sharpening down to sub-nanosecond risetimes in the nonlinear transmission lines (NLTL). The dominant mechanism of pulse sharpening is through generating a shockwave which occurs through saturation of the material's nonlinear permeability, energy dissipation at the traveling pulse front, and spin reversal in the magnetic material.[1,8] As the incident pulse traverses the NLTL, the nonlinear permeability undergoes saturation and the degree of saturation depends on the magnitude of the pulse. Consequently, the crest of the pulse front travels through a permeability of lower value than the base of the pulse front. The inverse relation between phase velocity and permeability allows the pulse front crest to "catch-up" to the base. Concurrently, the material is non-ideal, and therefore has associated losses. These losses result in energy dissipation across the pulse front, which aid in pulse steepening. With the application of an axial, static, biasing magnetic field, the magnetic moments begin to align in the same direction. The azimuthal magnetic field from the incident pulse switches the moments from their initial position into a new position establishing a spin reversal region which leads to magnetic moment switching aiding in the process of pulse sharpening.

Microwave generation occurs through damped gyromagnetic precession and can be accurately described by the Landau-Lifshitz-Gilbert equation (LLG). The normalized representation of the LLG is presented in Eq. (1). The LLG is a differential equation describing the magnetization dynamics taking place in the ferrite.

$$\frac{\partial \mathbf{m}}{\partial t} = -\gamma \mathbf{m} \times \mathbf{h}_{eff} + \alpha \mathbf{m} \times \frac{\partial \mathbf{m}}{\partial t}. \tag{1}$$

The first term on the right hand side of Eq. (1) represents the precessional motion of the magnetic moment, $\boldsymbol{m}$, around an effective magnetic field, $\boldsymbol{h_{eff}}$, while the second term is the relaxation term, governing the speed at which the moment

aligns or relaxes in the direction of the effective field. They gyromagnetic factor is represented by γ and the damping constant by α. The effective field consists of the exchange fields, anisotropy fields, demagnetizing fields, and external fields,[9] but due to the size and nature of the sample only demagnetizing fields and external fields are considered throughout design. The external fields consist of the axial biasing field and incident azimuthal field. Here, the axial biasing field is produced with a solenoid while the azimuthal field is due to the incident high voltage pulse. The biasing field initially aligns the magnetic moments in the axial direction while the azimuthal field pulls the moments away and switches them into the direction of the effective field.

III. EXPERIMENTAL SETUP

A high voltage dc power supply is utilized to charge a 2.5 nF capacitor bank to a user defined level, typically in the range of 20–40 kV, see Figure 1. Upon purging the pressurized cavity, the spark gap is over-volted and a damped Resistor-Inductor-Capacitor (RLC) signal propagates through a commercially available coaxial cable acting as a delay line before arriving at the NLTL input. After traversing the NLTL, the signal is terminated into a 50 Ω resistive load. The delay lines before and after the NLTL provide temporal isolation for diagnostic purposes in case of reflections between the source, load, and NLTL due to the dynamic impedance of the NLTL. Two high speed capacitive voltage probes are used as the main diagnostic tools, capturing the incident and output waveforms.

The NLTL consists of an aluminum or brass coaxial structure with nickel-zinc (NiZn) ferrites snugly fit along the inner conductor. Yttrium iron garnet (YIG), magnesium-zinc (MgZn), manganese-zinc (MnZn), and lithium ferrite have also been used in NLTL technologies, yet presently the most success has come from various compositions of NiZn. The high voltage levels and small space between conductors necessitates the use of an electrical insulator. Pressurized sulfur hexafluoride (SF_6 at 620 kPa) acts as the dielectric medium. Refer to Fig. 7 of Ref. 12 for a cross-sectional view of the constructed NLTL. A secondary dc power supply provides the necessary current through a solenoid wrapped around the outer conductor of the NLTL to produce the axially directed, magnetic biasing field.

The overall system impedance is designed for 50 Ω, assuming saturated permeability for the ferrite. Typically, the solenoid induced bias saturates the material, but if unsaturated, the incident azimuthal pulse quickly saturates the material. The line impedance is varied by varying the outer conductor of the NLTL as the ferrites are generally more difficult to fabricate and brass tubes are available in several sizes. The electric and magnetic field are highly dependent on the inner and outer conductor diameters as well as the ferrite sizes. Consequently, care must be taken in order to not exceed the voltage breakdown threshold of the ferrite or dielectric insulator as well as aiming to maintain a consistent magnetic field throughout the ferrimagnetic material. For a given driving current, the magnetic field has an inverse relation to the samples radius and thus the frequency of operation and bandwidth are affected by the ferrite's size.

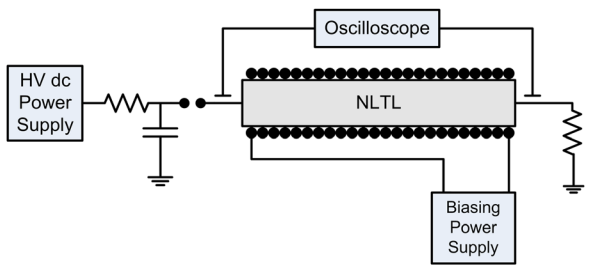

FIG. 1. Block diagram of the experimental setup. Capacitive voltage probes are used as diagnostics and are found at the input and output of the NLTL.

In the design stages, the frequency of operation is determined through traditional magnetization dynamics techniques, specifically the Smit and Beljers approximation for calculating the ferromagnetic resonance (FMR) frequency. The method utilizes the externally applied magnetic fields and demagnetizing fields calculated from the sample's dimensions. A MATLAB program takes an FFT of the output signal and an order of 10% accuracy has been achieved utilizing the traditional FMR techniques.

IV. RESULTS

Various ferrite material parameters significantly impact the efficiency of microwave generation. Two primaries are the magnetic and electric loss factors. While the dielectric loss value is typically stated in the data sheet of commercially available ferrites, the magnetic loss is generally unknown and needs to be measured in a separate experiment. FMR techniques have been utilized to measure the precession linewidth of several tested materials, and the FMR cavity resonance technique[10] was employed here. The ferrimagnetic material is sufficiently thinned, shaped into an ellipse, and placed in an X-band cavity resonator. The thin, elliptical shape allows the use of known demagnetizing fields and will not perturb the fields in the resonator. A 9.53 GHz source is used to excite the cavity resonator and a dc magnetic field is placed around the ferrite sample in order to saturate the material. The magnitude of the field is then swept, and the absorbed microwave power into the ferrite is recorded at various dc magnetic fields. When the magnetic field is such that resonance in the material is achieved, the power absorption peaks. The fundamental equation relating resonance and magnetic field is $\omega = \gamma \mathbf{H}_0$, where ω is the resonance frequency, γ is the gyromagnetic ratio, and $\mathbf{H}_0$ is the internal magnetic field. The FMR linewidth of the ferrite is recorded as the full width-half max (FWHM) of the absorbed power peak. This linewidth is directly related to the phenomenological damping factor found in LLG, Ref. 1. The waveforms listed in Figure 2 portray FMR spectra measured by Metamagnetics, Inc., for six materials with applied dc field, measured in kilo-Oersted, on the x-axis and the derivative of the absorbed power, measured in arbitrary units, listed on the y-axis.

To complement the FMR spectra are four measured waveforms from the NLTL output found in Figure 3. These waveforms represent a commercially available NiZn sample and three custom NiZn samples developed by Metamagnetics, Inc., narrow linewidth (<280 Oe) material have produced

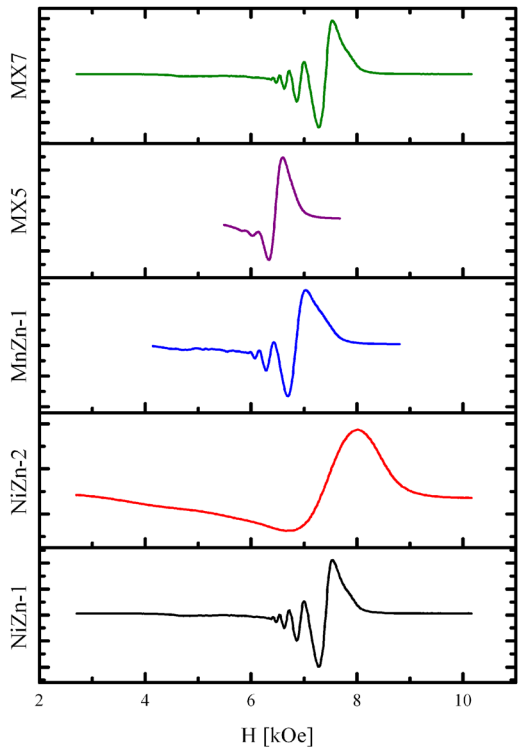

FIG. 2. FMR spectra of five different materials. The waveforms represent the derivative of absorbed power. The oscillatory nature prior to the main linewidth peak arises from spin-wave excitation.

microwave oscillations with narrower linewidths producing higher rf power and a longer duration of precession. A MnZn sample shows very narrow linewidth, but has resistivity 5–8 orders of magnitude lower than the NiZn samples. Due to the high electric loss, this MnZn sample proved to be too lossy and did not produce microwaves. In addition to low magnetic and dielectric loss tangents, the ferrite must have moderate values of initial relative permeability and saturation magnetization. The most successful ferrites have relative permeabilities in the upper hundreds and saturation magnetizations around 3500 G.

In addition to specific material parameters, the operational performance of the NLTL highly depends on the incident pulse and static biasing field magnitudes. Typical trends include increasing frequency with increasing incident pulse amplitude and decreasing frequency with increasing bias field.[11,12] This can be attributed to the total amount of azimuthal field seen by the ferrite. Since the NLTL geometry is coaxial, the acting propagation mode is transverse electric and magnetic (TEM) and thus an azimuthally-directed magnetic field is primary. Hence, the azimuthal component of the rotating magnetic moment couples to the TEM mode progressing down the line. Due to this coupling, it is evident that as the incident field increases, the projection of the rotating moment onto the azimuthal axis increases. In contrast, if the bias field increases, the azimuthal contribution decreases. Frequency versus bias field plots at varying incident voltage magnitudes can be found in Figure 4.

Expectedly, there exists optimal incident amplitude - bias combinations to achieve maximum rf output power, see Figure 5. At low bias field strengths, the majority of the magnetic moments are not aligned in the axial direction. Consequently, upon application of the azimuthal field, there exists a state of incoherent switching and precession between the moments, resulting in low rf power generation. In contrast, if the magnitude of the bias field is too large, the azimuthal field is too weak to significantly move the magnetic moments. Therefore, the azimuthal influence of the rotating magnetic moments is decreased.

Interestingly, the electrical delay of the system can be controlled with the NLTL. This is achieved through controlling the initial permeability of the ferrite with the biasing field. As the magnetic bias is increased to higher strengths, the material begins to saturate and the permeability decreases. Thus, the bias can effectively control the initial permeability seen by the incoming pulse front and therefore control the phase velocity of the wave. By altering the bias magnitude, length of bias, and ferrite, the NLTL can be actively tuned for specific delay times. This provides an

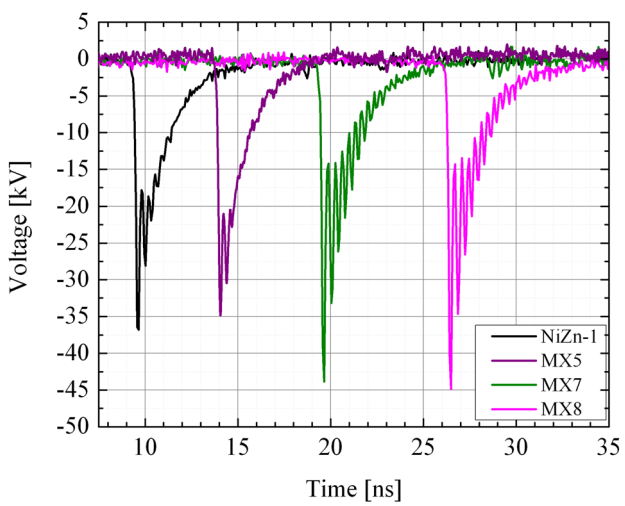

FIG. 3. NLTL Output waveforms for four different materials. The colors of each waveform correspond to the colors represented in Figure 2. The materials are NiZn-1, MX5, MX7, and MX8 (moving left to right). Each material has a different linewidth (first—260 Oe, second—280 Oe, third—130 Oe, and fourth—120 Oe).

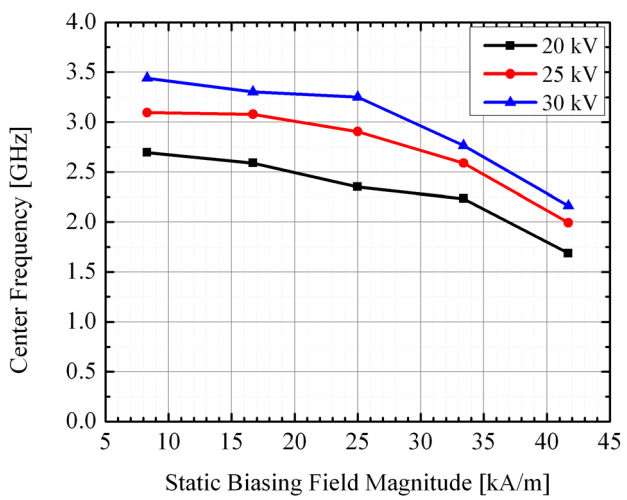

FIG. 4. Center frequency versus magnetic bias field for incident voltages 20 kV (black-□), 25 kV (red-○), and 30 kV (blue-Δ).

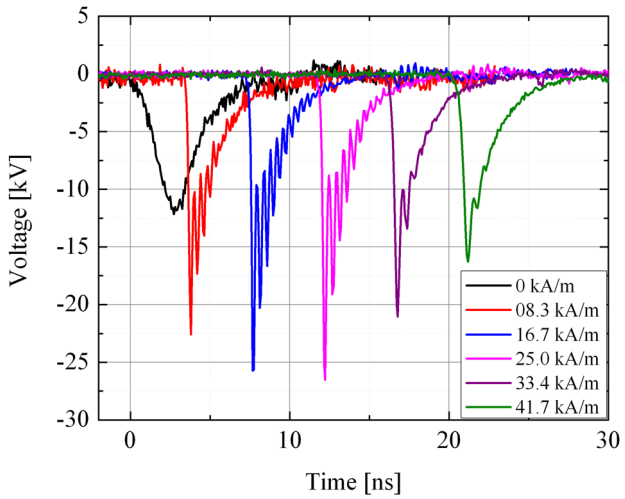

FIG. 5. NLTL outputs for 20 kV incident pulse magnitude and varying bias. The waveforms are arranged such that the bias field is increasing from left to right. For ease of viewing, the waveforms are time-shifted by 3 ns relative to each other.

exciting opportunity for NLTL integration into phased array systems. The delay can be altered through the use of one bias (controlling output power, frequency, and delay), the use of multiple biases on a single line (one for power/frequency, one for delay), or the use of multiple NLTLs and multiple biases. If using multiple biases for each NLTL, the bias located at the output portion of the NLTL determines the output power and frequency, while the electrical delay can be altered by a bias located on the front end of the NLTL.[11] At 20 kV, the total electrical delay was demonstrated to vary between 20.5 ns down to 9 ns. Figure 6 contains line plots of the changing electrical delay versus bias at various incident

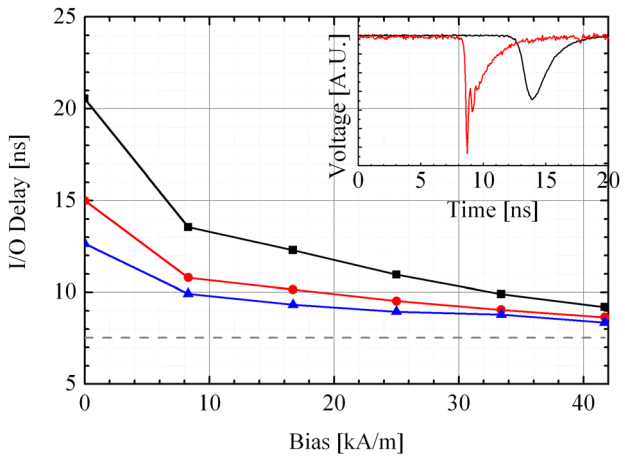

FIG. 6. The main figure contains the NLTL electrical delay versus biasing field at 20 kV (black-□), 25 kV (red-○), and 30 kV (blue-Δ). The gray line represents the calculated electrical length of the line when fully saturated. The inset figure contains waveforms for unbiased (0 kA/m, black, no oscillations) and fully biased (42 kA/m, red, oscillations present) outputs.

pulse magnitudes. The figure inset shows the dramatic delay change between unbiased and fully biased (presently 42 kA/m) lines. The dotted line represents the delay of full saturation which all lines asymptotically trend toward.

V. CONCLUSIONS

Nonlinear transmission lines have proven to be potential alternatives to traditional, vacuum-based high power microwave sources. Traditional magnetization dynamics techniques to predict frequency and measure microwave losses can be applied to NLTL design for determining operational frequency and expected material performance. Additionally, through altering the static bias, frequency tuning and system phasing can be achieved. Two material parameters have been determined with experimental results to verify the importance of magnetic and electric loss for microwave generation. This article shows the importance of careful design to achieve large magnetic fields in the ferrite, tailored magnetic field differential for bandwidth control, and choice of material for optimal microwave generation.

ACKNOWLEDGMENTS

This work was supported by the U.S. Office of Naval Research (ONR).

[1]I. Katayev, *Electromagnetic Shock Waves* (Iliffe, 1966).
[2]J. Dolan, "Simulation of shock waves in ferrite-loaded coaxial transmission lines with axial bias," J. Phys. D: Appl. Phys. **32**, 1826 (1999).
[3]I. Romanchenko, V. Rostov, V. Gubanov, A. Stepchenko, A. Gunin, and I. Kurkan, "Repetitive sub-gigawatt rf source based on gyromagnetic nonlinear transmission line," Rev. Sci. Instrum. **83**, 074705 (2012).
[4]J. Darling and P. Smith, "High power pulsed rf generation from nonlinear lumped element transmission lines (NLETLs)," University of Oxford, Technical Presentation, given at the University of New Mexico, 2008.
[5]N. Seddon, C. Spikings, and J. Dolan, "RF pulse formation in nonlinear transmission lines," in *IEEE 34th International Conference on Plasma Science*, Albuquerque, NM, (2007).
[6]H. Shi, C. W. Domier, and N. C. Luhmann, "A monolithic nonlinear transmission line system for the experimental study of lattice solitons," J. Appl. Phys. **78**, 2558 (1995).
[7]M. Jamshidifar, G. Spickermann, H. Schafer, and P. Haring Bolivar, "200-GHz bandwidth on wafer characterization of CMOS nonlinear transmission line using electro-optic sampling," Microwave Opt. Technol. Lett. **54**(8), 1858 (2012).
[8]M. Weiner and L. Silber, "Pulse sharpening effects in ferrites," IEEE Trans. Magn. **17**(4), 1472 (1981).
[9]I. Mayergoyz, G. Bertotti, and C. Serpico, *Nonlinear Magnetization Dynamics in Nanosystems* (Elsevier, 2008).
[10]A. Geiler, private communication (2011).
[11]J. -W. B. Bragg, J. C. Dickens, and A. A. Neuber, "Nonlinear transmission line performance under various magnetic bias environments," in *Directed Energy Professional Society Annual Directed Energy Symposium*, La Jolla, CA, (2011).
[12]J.-W. Bragg, W. W. Sullivan III, D. Mauch, J. C. Dickens, and A. A. Neuber, "Compact pulsed power system realized through integrated SiC photoconductive semiconductor switch and gyromagnetic nonlinear transmission line," Rev. of Sci. Instr. (submitted).